DOI: 10.1002/ejic.200600452

A Binuclear Isocyanide Azadithiolatoiron Complex Relevant to the Active Site of Fe-Only Hydrogenases: Synthesis, Structure and Electrochemical Properties

Jun Hou,[a] Xiaojun Peng,*[a] Jifeng Liu,[b] Yunling Gao,[b] Xing Zhao,[a] Shang Gao,[a] and Keli Han[b]

Keywords: Bioinorganic chemistry / Density functional calculations / Hydrogenases / Iron / Isocyanide ligands

An aromatic isocyanide-substituted diiron complex **5** has been synthesized as a mimic for the active site of Fe-only hydrogenases. Its structure has been fully characterized by X-ray crystallography. The 4-iodophenylisocyanide ligands in **5** are in the basal positions and are nearly parallel to each other, with π–π stacking interactions. Four isomeric geometries of complex **5** have been optimized by DFT calculations, and the electrochemical properties of **5** have been investigated by cyclic voltammetry in the absence and presence of *p*-toluenesulfonic acid (HOTs). Analysis of the cyclic voltammetric curve indicates that the reduction event at about –1.43 V is electrocatalytically active to proton reduction. This potential is more positive than that of any functionalized propanedithiolatodiiron complex.

Introduction

Proton reduction to hydrogen in proteins, according to the reaction $2H^+ + 2e^- \rightleftarrows H_2$, is catalyzed in a highly efficient manner by Fe-only hydrogenases ([Fe]H_2ases), with rates in the range of 6000–9000 per second.[1–3] Because of this significant efficiency, [Fe]H_2ases have drawn considerable attention from chemists in the past few years.

As revealed by a combination of X-ray crystallography[4,5] and IR spectroscopy,[6,7] the active site of [Fe]H_2ases is comprised of a 2Fe2S subunit linked to a 4Fe4S cluster by a cysteinyl-S bridge. The 4Fe4S unit is probably responsible for electron transfer while the 2Fe2S subsite is utilized as a catalytic center for hydrogen formation and activation. The two iron atoms in the 2Fe2S subunit are bridged by the sulfur atoms of a propanedithiolato (PDT) ligand and bear the biologically unusual ligands CO and CN^-. Theoretical studies support the assignment of the bridging ligand as having the structure $–SCH_2NCH_2S–$ (ADT),[8,9] and the nitrogen heteroatom likely plays an important role in H_2 production in the natural system.

The unique structure of the active site has inspired bioinorganic chemists to synthesize structural and functional models.[10–15] Numerous biomimetic models of the PDT-[16] or ADT-bridged[17,18] all-carbonyl diiron complexes, as well as of their isocyanide,[19,20] thioether,[21–23] and phosphane/cyano-substituted[24,25] analogues have been prepared. Recently, Pickett and co-workers have reported their assembly by linking of an $[Fe_4S_4]$ cluster to a diiron unit, which offers the prospect of understanding the catalytic mechanisms of [Fe]H_2ases.[26] Rauchfuss et al. have developed syntheses of mixed-ligand diferrous dithiolate complexes by the oxidative decarbonylation of diiron dithiolates,[27,28] and Darensbourg and co-workers have described the electrocatalytic production of H_2 by PDT-bridged diiron derivatives [(μ-PDT)$Fe_2(CO)_4(PR_3)_2$] in the presence of the weak acid HOAc.[29,30] Rauchfuss et al. have demonstrated that the mixed-ligand substituted diiron system [(μ-PDT)$Fe_2(CO)_4$-$PMe_3(CN)]^-$ is an electrocatalyst for H_2 production with the strong acid *p*-toluenesulfonic acid (HOTs).[31,32] However, relatively more negative potentials are required to drive the reduction of protons to H_2 with these synthetic systems. Sun and co-workers have reported that the introduction of nitrogen in the ADT bridge shifts the reduction potential to a more positive value.[33] Thus, the synthesis of functionalized azadithiolatodiirons may be an alternative in the search for synthetic catalysts with [Fe]H_2ase-like capability. Although ADT-bridged diiron complexes have been extensively studied,[34–39] to the best of our knowledge there is no report on the electrocatalytic reduction of protons catalyzed by functionally substituted azadithiolatodiiron derivatives in the literature to date. With this in mind, we present here a binuclear isocyanide azadithiolatoiron complex **5** in which the isocyanide ligand was chosen because it can be used as a surrogate for the relevant CN^- without complicating the reactivity of the cyanide nitrogen in catalytic reactions.[19,20] We describe the preparation, structural charac-

[a] State Key Laboratory of Fine Chemicals, Dalian University of Technology,
Dalian 116012, P. R. China
Fax: +86-411-8899-3906
E-mail: pengxj@dlut.edu.cn
[b] State Key Laboratory of Molecular Reaction Dynamics, Dalian Institute of Chemical Physics, Chinese Academy of Science,
Dalian 116022, P. R. China
Supporting information for this article is available on the WWW under http://www.eurjic.org or from the author.

terization, and DFT calculations of the possible isomers of **5**, as well as the electrochemical properties of **5** in the absence and presence of the moderately strong acid HOTs.

Results and Discussion

Synthesis and Spectroscopic Characterization of Complexes 3 and 5

The complex [{(μ-SCH_2)$_2$N(4-$CH_3C_6H_4$)}$Fe_2(CO)_6$] (**3**) was prepared by a similar procedure to that reported by Rauchfuss (Scheme 1).[34] The lithium salt of hexacarbonyldisulfidodiiron (**1**),[40] freshly derived from [(μ-S)$_2$$Fe_2$-$(CO)_6$], was treated with *N*,*N*-bis(chloromethyl)-4-methylaniline (**2**) to give complex **3** in moderate yield. The synthesis of [{(μ-SCH_2)$_2$N(4-$CH_3C_6H_4$)}$Fe_2(CO)_4$(4-IC_6H_4NC)$_2$] (**5**) from complex **3** and 4-iodophenylisocyanide (**4**) turned out to be a challenge. Treatment of **3** with two equivalents of **4** in CH_2Cl_2 or CH_3CN solution afforded complex **5** in very low yield, and attempts to afford disubstituted isocyanide derivative **5** in refluxing MeCN solution by Rauchfuss' protocol[19] were unsuccessful because **4** is thermally unstable. However, reaction of complex **3** with **4** in CH_3CN/CH_2Cl_2 (2:1, v/v) solution in the presence of the decarbonylating agent $Me_3NO{\cdot}2H_2O$ at room temperature gave the desired product **5** in reasonable yield after purification by column chromatography on silica gel. Complexes **3** and **5** are stable to air in the solid state but moderately sensitive in solution.

Complexes **3** and **5** were characterized by IR and ^{1}H and ^{13}C NMR spectroscopy and mass spectrometry. The IR spectrum of complex **3** in CH_2Cl_2 shows three major bands in the CO region at 2071, 2030, and 2000 cm^{-1}, in agreement with those of other azadithiolatodiiron derivatives.[34–36] The IR spectrum of complex **5** in CH_2Cl_2 exhibits NC bands at 2122 and 2094 cm^{-1} and CO bands at 1996, 1980, and 1950 cm^{-1}. Compared with the signals of **3**, the stretching frequencies of CO are shifted to lower wavenumbers by about 50 cm^{-1} on average, consistent with the better electron-donating ability of 4-iodophenylisocyanide with respect to the CO ligand. This indicates that the introduction of aromatic isocyanide ligands to the diiron center increases the electron density of the Fe–Fe bond.

Structures of Complexes 3 and 5

The solid-state structures of **3** and **5** were determined by X-ray diffraction. The structure of **3** is shown in Figure 1 and selected bond lengths and bond angles are listed in Table 1. The 2Fe2S unit has a pseudo-square-pyramidal geometry, similar to those of previously reported azadithiolatodiiron derivatives.[34–36] The 4-methylphenyl ring slants towards the Fe(2)$(CO)_3$ unit, and the axis containing N(1), C(9), C(12), and C(15) atoms is nearly parallel to the apical C(6)O(6) ligand on the Fe(2) atom. It is noteworthy that the C(6)–Fe(2)–Fe(1) angle is about 7° larger than the C(2)–Fe(1)–Fe(2) angle, thus indicating an interaction between the arene group and Fe(2)$(CO)_3$ unit. The Fe–Fe distance of 2.5090(10) Å agrees well with those found in other (μ-ADT)$Fe_2(CO)_6$ structures.

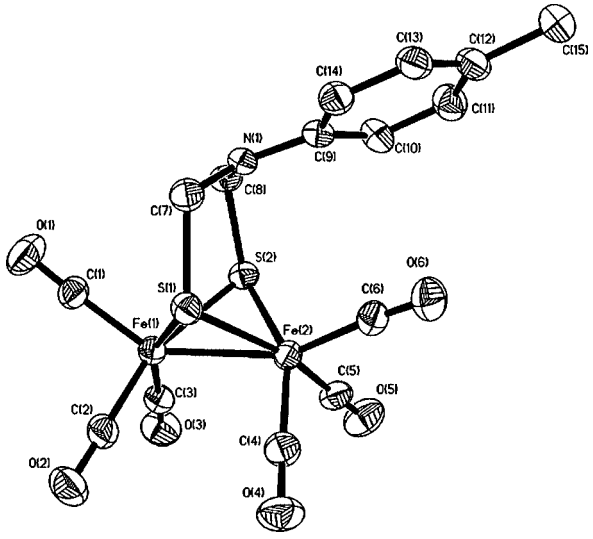

Figure 1. ORTEP view of **3** (ellipsoids at 30% probability level).

The molecular structure of **5** in the solid state is displayed in Figure 2 and selected lengths and angles are listed in Table 2. Like the "parent" **3**, the central 2Fe2S unit of **5** adopts a face-shared bi-octahedral structure. The Fe–Fe bond length of 2.5121(11) Å is somewhat longer than that observed in **3** and is similar to that found in an isocyanide-substituted PDT-bridged diiron complex.[20] This indicates that the metal–metal distance in diiron(I) compounds is

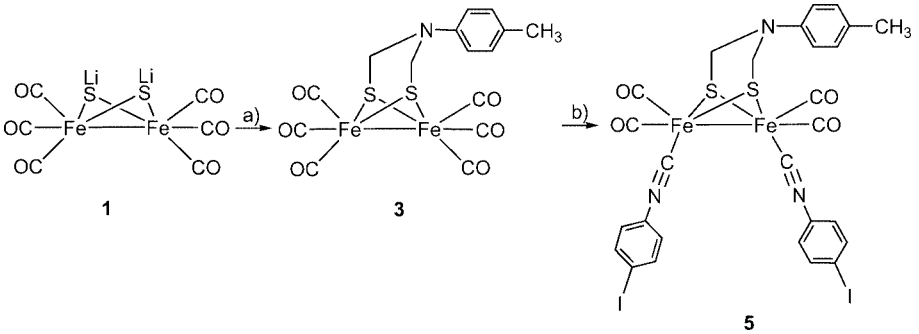

Scheme 1. a) $(ClCH_2)_2N(4\text{-}CH_3C_6H_4)$ (**2**), thf, –78 °C, 2 h; b) 4-iodophenyl isocyanide (**4**), $Me_3NO{\cdot}2H_2O$, CH_3CN/CH_2Cl_2 (1:1, v/v), room temp., 48 h.

Table 1. Selected bond lengths [Å] and angles [°] for **3**.

Fe(1)–Fe(2)	2.5090(10)	Fe(1)–S(1)–Fe(2)	67.44(4)
Fe(1)–S(1)	2.2614(14)	Fe(1)–S(2)–Fe(2)	67.28(4)
Fe(1)–S(2)	2.2626(15)	S(1)–Fe(1)–S(2)	85.05(5)
Fe(2)–S(1)	2.2585(14)	S(1)–Fe(2)–S(2)	85.02(5)
Fe(2)–S(2)	2.2666(15)	C(7)–S(1)–Fe(1)	110.7(2)
Fe(1)–C(1)	1.797(6)	C(8)–S(2)–Fe(1)	107.59(19)
Fe(1)–C(2)	1.783(6)	C(1)–Fe(1)–C(3)	99.3(3)
Fe(1)–C(3)	1.797(6)	C(3)–Fe(1)–C(2)	90.2(3)
N(1)–C(7)	1.420(8)	C(2)–Fe(1)–C(1)	99.3(3)
N(1)–C(8)	1.411(8)	C(1)–Fe(1)–S(1)	101.99(19)
N(1)–C(9)	1.413(7)	C(1)–Fe(1)–S(2)	99.4(2)
		C(9)–N(1)–C(8)	121.3(5)
		C(9)–N(1)–C(7)	122.3(5)
		C(7)–N(1)–C(8)	113.8(5)

slightly affected by the nature of terminal ligands with a better electron-donating ability. The p-π conjugation between the 4-methylphenyl ring and the bridging N p orbital is somewhat weakened, therefore the bridging N atom is not in the plane defined by the atoms C(12), C(10), and C(19). The sum of the C–N–C angles around N(3) is 354°. The 4-methylphenyl ring in an axial position is approximately parallel to the apical carbonyl ligand C(22)O(3) on the Fe(2) site, as found in **3**. The C(20)–Fe(2)–Fe(1) angle in **5** [156.5(2)°] is enlarged by about 3.6° compared to the corresponding angle [C(6)–Fe(2)–Fe(1)] in **3** [152.83(19)°], thus suggesting the effect of the phenylisocyanide ligands on the diiron unit. The C(7)–N(1)–C(4) angle [177.3(7)°] on the Fe(1) unit is relatively linear, whereas the C(21)–N(2)–C(23) angle [168.1(7)°] on the Fe(2) unit is slightly bent. The bending at the N(2) atom is probably due to a steric influence of the bulky isocyanide ligands. The average Fe–C(N) distance of 1.846(6) Å is slightly larger than that of Fe–C(O) [av. 1.7805(7) Å]. It is interesting to note that the two phenylisocyanide ligands in the basal positions on each iron unit are nearly parallel to each other, thus indicating a crystal stacking interaction between them. Figure 3 displays the packing view along the *b* axis. It shows π–π stacking interactions of the 4-iodophenylisocyanide ligands within the column. Complex **5** is unusual compared to related diiron isocyanide complexes where the two isocyanide ligands are in apical positions in the solid state and are not parallel to each other.[20]

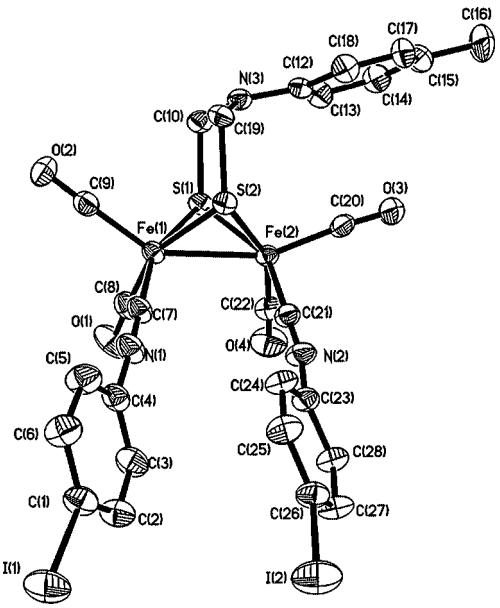

Figure 2. ORTEP view of **5** (ellipsoids at 30% probability level).

Table 2. Selected bond lengths [Å] and angles [°] for **5**.

Fe(1)–Fe(2)	2.5121(11)	Fe(1)–S(1)–Fe(2)	67.29(5)
Fe(1)–S(1)	2.2642(16)	Fe(1)–S(2)–Fe(2)	67.25(5)
Fe(1)–S(2)	2.2698(17)	S(1)–Fe(1)–S(2)	84.93(6)
Fe(2)–S(1)	2.2698(17)	S(1)–Fe(2)–S(2)	84.87(6)
Fe(2)–S(2)	2.2668(17)	C(10)–S(1)–Fe(1)	107.6(2)
Fe(1)–C(7)	1.846(6)	C(19)–S(2)–Fe(1)	109.3(2)
Fe(1)–C(8)	1.758(8)	C(9)–Fe(1)–C(8)	101.1(3)
Fe(1)–C(9)	1.806(7)	C(8)–Fe(1)–C(7)	90.1(3)
N(1)–C(7)	1.158(8)	C(7)–Fe(1)–C(9)	100.1(3)
N(1)–C(4)	1.409(8)	C(9)–Fe(1)–S(1)	99.8(2)
N(2)–C(21)	1.165(8)	C(9)–Fe(1)–S(2)	101.5(2)
N(2)–C(23)	1.397(8)	C(12)–N(3)–C(19)	121.0(5)
N(3)–C(12)	1.396(7)	C(12)–N(3)–C(10)	121.7(5)
N(3)–C(10)	1.398(8)	C(10)–N(3)–C(19)	111.5(5)
N(3)–C(19)	1.434(8)	C(7)–Fe(1)–S(1)	159.8(2)
I(1)–C(1)	2.092(7)	C(7)–Fe(1)–S(2)	87.6(2)
		N(1)–C(7)–Fe(1)	178.9(7)
		N(2)–C(21)–Fe(2)	177.7(6)
		C(4)–N(1)–C(7)	177.3(7)
		C(23)–N(2)–C(21)	168.1(7)

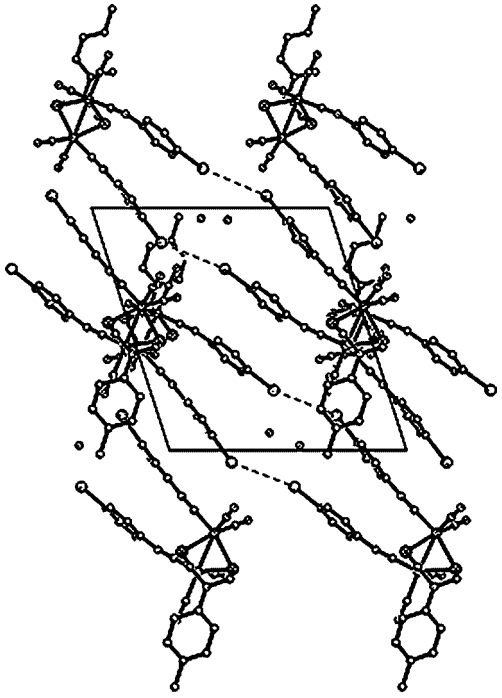

Figure 3. Crystal packing diagram for **5** viewed along the *b* axis. Thermal ellipsoids are drawn at the 50% possibility level.

In contrast to the solid structure, complex **5** exists as isomers, with two different CN stretching frequencies at 2122 and 2094 cm^{-1}, respectively, in solution. This phenomenon is analogous to that described for the related isocyanide

derivative $[(\mu\text{-}S_2C_3H_6)Fe_2(CO)_4(t\text{Bu}_4\text{NC})_2]$.[20] In general, complexes of this type can share several isomeric geometries in solution on the basis of ligands in apical or axial positions.

DFT Structure Calculations for 5

To gain insight into the possible isomeric structures based on the different positions of the two isocyanide ligands, the possible geometries of **5** were optimized by using DFT methods. Theoretically, there are four possible isomers for doubly substituted diiron complexes, that is ap/ap, ba/ap, ba/ba, and ap/ba configuration modes. Four optimized structures of the relevant isomers of **5** are shown in Figure 4. Selected geometrical parameters are summarized in the Supporting Information. A comparison of these structures reveals that the Fe–Fe distance is affected by the arrangement of the CO and 4-IC_6H_4NC groups. This effect can be partly attributed to the competition between π-acceptors for the π electrons. The crystallographically characterized isomer **5** is analogous to the computed complex **5.4**. Notably, the bond lengths and angles are in good agreement with the X-ray data and the two phenylisocyanide groups in the basal positions are close to parallel.

From the relative energies of the four isomers shown in Table S1, it can be seen that in the monomer case the stabilization sequence of the four conformations for **5** in the gas phase is **5.2** > **5.3** > **5.4** > **5.1**. When considering the solvent effect, we found that the stabilization sequence changes and isomer **5.4** becomes the most stable one in CCl_4 solution at 298 K. The stabilization sequence in CCl_4 solution is **5.4** > **5.1** > **5.3** > **5.2**. Theoretical calculations show an important role for the solvent effect on structure selection

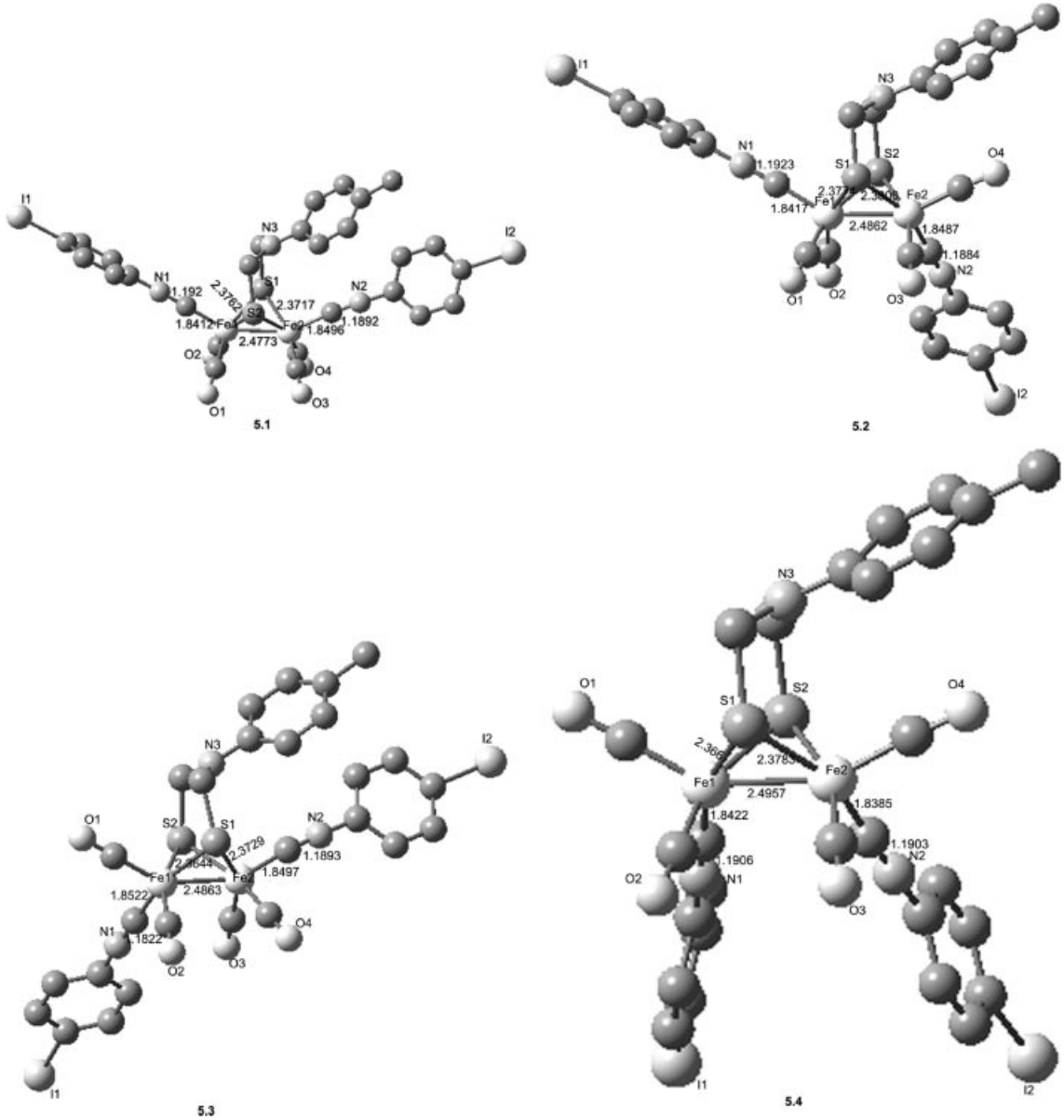

Figure 4. DFT-optimized structures of the four isomers of complex **5**. Selected bond lengths [Å] are given.

during the crystallization of complex **5**. The energy difference between isomers is less than 15 kJ mol^{-1}, which means that isomers of complex **5** can interchange easily.

Electrochemistry of Complexes 3 and 5

The ADT-bridged diiron hexacarbonyl compounds [(μ-ADT)$Fe_2(CO)_6$][33,35] and their phosphane-substituted derivatives[36] have been reported to undergo an electrochemically quasi-reversible/irreversible reduction at moderately negative potentials depending on the electron-donating abilities of the ligands on the diiron core. The cyclic voltammograms of complexes **3** and **5** shown in Figure 5 were recorded in CH_3CN solution (with 0.1 M nBu$_4$NPF$_6$ as electrolyte) and proceed, as indicated, in the cathodic direction. Complexes **3** and **5** display a quasi-reversible reduction peak and an irreversible oxidation wave, respectively. By comparison with electrochemical data for PDT-bridged diiron complexes[29,30] and ADT-bridged diiron analogues,[33,35,36] the reduction peaks at –1.55 V for **3** and –1.70 V for **5** vs. Fc^+/Fc can be assigned to the one-electron reduction process of Fe^IFe^I to Fe^IFe^0. The oxidation peaks at 0.55 V for **3** and at 0.13 V for **5** can be attributed to a net one-electron process, but further work is needed to establish this aspect of the electrochemistry. In comparison to that of the parent complex **3**, the reduction potential of **5** shifts by about 0.15 V to a more negative value, and the oxidation peak shifts by about 0.42 V to a less positive value. These shifts of potential indicate that the introduction of 4-iodophenylisocyanide ligands in **5** makes the reduction of the iron core more difficult and the oxidation easier, which is consistent with the better donor capacity of 4-iodophenylisocyanide relative to CO. A similar trend in the diiron analogue [{(μ-$SCH_2)_2$N(4-BrC_6H_4)}$Fe_2(CO)_5$-PPh_3] has been reported by Sun and co-workers.[36]

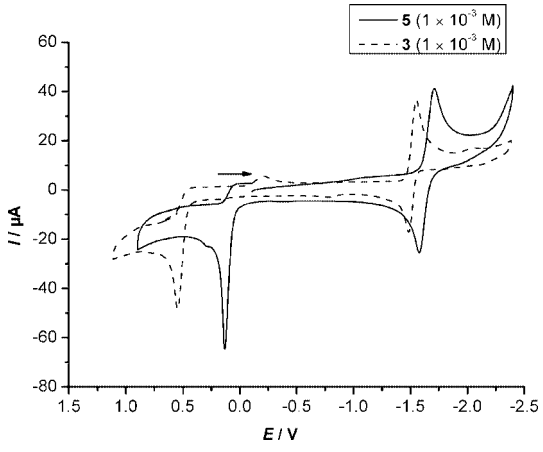

Figure 5. Cyclic voltammograms of **3** and **5** (1 mM) in 0.1 M nBu$_4$NPF$_6$/CH_3CN solution at a potential scan rate of 100 mV s^{-1}.

Electrocatalytic Proton Reduction in CH_3CN Solution

The electrocatalytic proton reduction by **5** was investigated by cyclic voltammetry in the presence of the moderately strong acid HOTs. The cyclic voltammogram recorded in CH_3CN solution at different acid concentrations (0–4 mM) is shown in Figure 6. Upon addition of 1 mM of HOTs, two new reduction peaks were observed at around –1.20 and –1.43 V. As can be seen in Figure 6, the current height of the reduction peak around –1.20 V displays a slight increase with an increase of acid concentration, while the reduction wave at around –1.43 V shows a significant electrocatalytic response. The current intensity of this reduction peak gradually increases and the potential is shifted to a relatively more negative value with increasing acid concentration. The current intensity (I_{pc}) of this reduction displays a linear increase with an increase of the concentration of HOTs, as shown in Figure 7. The steeper slope is indicative of the sensitivity of the reduction to acid concentration. These features are typical of a catalytic proton reduction process.[41] At [H^+]/[**5**] ≥ 5, the reduction peak at around –1.70 V disappears and the height of the reduction event around –1.43 V also increases and its potential shifts to a more negative value (Figure S1). We conclude that the reduction peak around –1.43 V displays an electrocatalytic response to proton reduction. The reduction peak around –1.20 V may be the reduction process of a protonated product, and further work is needed to define it properly. To further confirm the catalytic activity of **5** around –1.43 V, bulk electrolysis of solutions of 2 mM **5** with 50 mM HOTs was performed at –1.50 V. After passage of 20 C of charge through the cell, a sample of gas was collected and analyzed. Analysis by gas chromatography showed the gas evolved during electrolysis to be H_2.

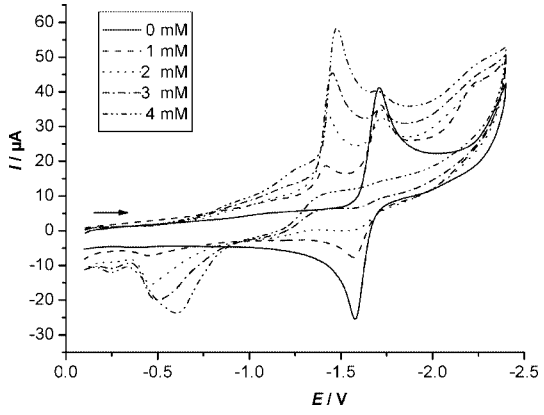

Figure 6. Cyclic voltammograms of **5** (1 mM) with 0–4 mM HOTs in 0.1 M nBu$_4$NPF$_6$/CH_3CN solution at a potential scan rate of 100 mV s^{-1}.

Electrocatalytic H_2 production by the cyano/phosphane-substituted diiron derivative [(μ-PDT){$Fe(CO)_2PMe_3$}-{$Fe(CO)_2CN$}]$^-$ has been reported by Rauchfuss and coworkers under similar acid conditions (HOTs).[31,32] The potential for the reduction of protons was found to be E_p^{red} = –1.2 V vs. Ag/AgCl (corresponding to –1.69 V vs. Fc^+/Fc),[42] which means that the potential of complex **5** is shifted by about 260 mV to a more positive value. Compared with all other functionalized PDT-bridged substituted diiron compounds,[29,30] complex **5** also has a con-

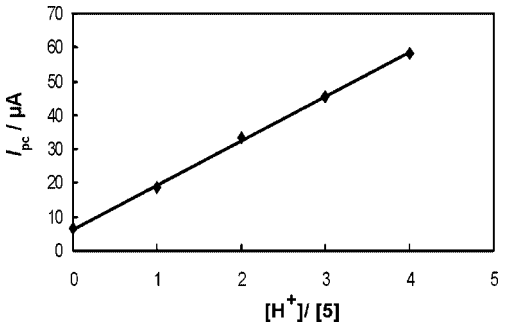

Figure 7. Dependence of current intensity of the reduction events of **5** (1 mM) around –1.43 V on concentration of HOTs.

siderably more positive potential of proton reduction. A reasonable interpretation for this is that the utilization of the basicity of the ADT heteronitrogen atom[43] and the introduction of isocyanide ligands shift the potential to a more positive value and therefore makes the reduction of protons remarkably easier.

Upon addition of acid, an irreversible event is observed at around –0.6 V on the reverse scan. This presumably results from a reduction-derived decomposition product.[29,44]

Conclusions

The binuclear aromatic isocyanide substitute [{(μ-SCH_2)$_2$-N(4-$CH_3C_6H_4$)}$Fe_2(CO)_4$(4-IC_6H_4NC)$_2$] (**5**) has been prepared as an active site model of iron-only hydrogenases. Both **5** and its parent complex **3** have been fully characterized by X-ray diffraction. The structure of **5** is highly unusual in that the two phenylisocyanide ligands are in basal positions and are nearly parallel to each other. This suggests that steric or crystal packing forces control the stereochemistry of CO and the aromatic isocyanide ligands. The introduction of the isocyanide ligands in **5** makes the CO stretching frequencies shift to lower values. These lower values of $\nu_{(CO)}$ indicate that the diiron core is more electron-rich, which is also consistent with the shift of the reduction potential of **5** to a more negative value.

The results of DFT calculations show that the binuclear active site of **5** has four possible isomers. One of these was isolated and characterized crystallographically because of the potential for isomeric complexity. It is likely that the π–π stacking interaction between molecules of complex **5** makes the isomer **5.4** stable enough to crystallize from solution.

On the basis of electrochemical analyses of **5**, the reduction peak around –1.43 V is electrocatalytically active in the presence of HOTs. The iodo functionality in **5** could be used for further elaboration by incorporating a redox species. This offers a possibility of linking a ruthenium photosensitizer to the azadithiolatodiiron system **5** in an attempt to produce H_2 by action of light.[15] Further experimental efforts in these directions are underway.

Experimental Section

Reagents and Instrumentation: All reactions and operations were carried out under N_2 using standard Schlenk techniques. All solvents were dried and distilled prior to use according to standard methods. Tetrahydrofuran was purified by distillation under N_2 from sodium/benzophenone. Acetonitrile was distilled once from CaH_2 and once from P_2O_5 and freshly distilled from CaH_2 prior to use. Dichloromethane was distilled from P_2O_5 under N_2. The following materials were commercially available reagents and used without further purification: paraformaldehyde, 4-methylaniline, and 4-iodoaniline. $LiEt_3BH$ was purchased from Aldrich and used as received. *N*,*N*-Bis(chloromethyl)-4-methylaniline (**2**), [(μ-S)$_2$-$Fe_2(CO)_6$], [(μ-LiS)$_2Fe_2(CO)_6$] (**1**), and 4-iodophenylisocyanide (**4**) were synthesized according to the literature procedures.[34,40,45,46]

Infrared spectra were recorded with a FT-IR spectrophotometer. ^1H and ^{13}C NMR spectra were recorded on a Varian INOVA 400 NMR spectrometer. Mass spectra were recorded with a HP 100 MSD. HR mass spectra were recorded on a Q-TOF mass spectrometer or a GC-TOF instrument (Micromass).

Synthesis of [{(μ-SCH_2)$_2$N(4-$CH_3C_6H_4$)}$Fe_2(CO)_6$] (3): $LiEt_3BH$ solution (1 M solution in thf, 2.9 mL, 2.9 mmol) was added to a solution of [(μ-S)$_2Fe_2(CO)_6$] (500 mg, 1.45 mmol) in thf (30 mL) by syringe at –78 °C over 30 min. A solution of *N*,*N*-bis(chloromethyl)-4-methylaniline (**2**) in thf (20 mL) was added to the resulting green solution, causing an immediate change of color to dark red. After stirring for 2 h at –78 °C and for 1 h at room temperature, the solvent was removed in vacuo and the resulting dark-red solid was purified by column chromatography on silica gel using CH_2Cl_2/hexane (1:10) as eluent to afford a dark-red solid. Yield: 57% (recrystallized from CH_2Cl_2/hexane). ^1H NMR (400 MHz, $CDCl_3$): δ = 7.12 (s, 2 H), 6.66 (s, 2 H), 4.31 (s, 4 H), 2.28 (s, 3 H) ppm. ^{13}C NMR (100 MHz, $CDCl_3$): δ = 209.0, 207.2, 142.8, 130.6, 130.2, 116.3, 53.6, 50.2, 19.5 ppm. IR (CH_2Cl_2): $\nu_{(CO)}$ = 2071, 2030, 1999 cm^{-1}. MS (API-ES): (*m*/*z*): 478 $[M + H]^+$. HR-MS (ESI) calcd. for $[M + H]^+$: 477.8805; found 477.8793.

Synthesis of [{(μ-SCH_2)$_2$N(4-$CH_3C_6H_4$)}$Fe_2(CO)_4$(4-IC_6H_4NC)$_2$] (5). Method A: A solution of complex **3** (1 g, 2.09 mmol) in CH_3CN (30 mL) was treated with a solution of 4-IC_6H_4NC (0.96 g, 4.19 mmol) in CH_2Cl_2 (30 mL) at room temperature, followed by the addition of $Me_3NO{\cdot}H_2O$ (0.465 g, 4.19 mmol) in CH_3CN (20 mL). The solution immediately turned dark purple, and after 5 h the color had changed again to dark red. The mixture was stirred at room temperature for 48 h and TLC showed the reaction was complete. The solvent was removed in vacuo and the dark-red residue was purified by column chromatography on silica gel eluting with hexane/dichloromethane (5:1). Two main bands were observed: the first red band, containing [{(μ-SCH_2)$_2$N(4-$CH_3C_6H_4$)}-$Fe_2(CO)_5$(4-IC_6H_4NC)] [IR (CH_2Cl_2): ν_{CN} = 2124 cm^{-1}, ν_{CO} = 2040, 2000, 1975 cm^{-1}], was collected with around 600 mL of eluent, and the second red band (**5**), with a further 1000 mL of eluent, was collected to give the red product **5**. Yield: 640 mg (34%) (recrystallized from CH_2Cl_2/hexane). ^1H NMR (400 MHz, [D_6]acetone): δ = 7.77 (d, *J* = 8.4 Hz, 2 H), 7.11 (d, *J* = 8.4 Hz, 2 H), 7.03 (d, *J* = 8.0 Hz, 2 H), 6.77 (d, *J* = 8.0 Hz, 2 H), 4.38 (s, 4 H), 2.14 (s, 3 H) ppm. ^{13}C NMR (100 MHz, $CDCl_3$): δ = 211.5 (CN), 205.5, 202.5 (CO), 147.0, 143.5, 138.6, 130.2, 128.7, 127.5, 115.8, 93.3, 49.8, 20.5 ppm. IR (CH_2Cl_2): $\nu_{(CN)}$ = 2122, 2094 cm^{-1}; $\nu_{(CO)}$ = 1996, 1980, 1950 cm^{-1}. HR-MS (EI) calcd. for $[M^+]$: 878.7605; found 878.7601.

Methods B: A 100-mL Schlenk flask was charged with [{(μ-SCH_2)$_2$-N(4-$CH_3C_6H_4$)}$Fe_2(CO)_6$] (**3**; 500 mg, 1.04 mmol) and 4-IC_6H_4NC

(479 mg, 2.09 mmol), 50 mL of CH_2Cl_2 was added to this flask, and the solution was stirred 48 h at room temperature. The solvent was removed in vacuo and the residue was purified by column chromatography on silica gel, eluting with hexane/dichloromethane (5:1). The first band, containing a large quantity of the monoisocyanide-substituted product, was collected with about 800 mL of eluent, and the second red band containing **5** with a further 200 mL. Yield of **5**: 92 mg (10%; recrystallized from CH_2Cl_2/hexane).

X-ray Structure Determinations: The single-crystal X-ray data were collected with a Siemens SMART CCD diffractometer for **3**, while the measurement for **5** was performed on a Siemens P4 four-circle diffractometer. In all cases, the data were collected at 293 K using graphite monochromated Mo-K_α radiation (λ = 0.71073 Å) in the ω–2θ scan mode. Data processing was accomplished with the SAINT processing program.[47] Intensity data were corrected for absorption with empirical methods. The structures of complexes **3** and **5** were solved by direct methods and refined on F_o^2 against full-matrix least-squares with the SHELXTL 97 program package.[48] All non-hydrogen atoms were refined anisotropically. Hydrogen atoms were located by geometrical calculation, but their positions and thermal parameters were fixed during the structure refinement. A summary of the crystallographic data and structural determinations for **3** and **5** is provided in Table 3.

Table 3. X-ray crystallographic data for **3** and **5**.

	3	**5**
Formula	$C_{15}H_{11}Fe_2NO_6S_2$	$C_{27}H_{23}Fe_2I_2N_3O_6S_2$
M_r [g mol^{-1}]	475.05	915.12
λ [Å]	0.71073	0.71073
Crystal system	triclinic	monoclinic
Space group	$P\bar{1}$	$P2_1/c$
a [Å]	7.8394(3)	13.3600(8)
b [Å]	9.6753(3)	21.6360(14)
c [Å]	12.4508(3)	12.4395(8)
α [°]	99.2350(10)	90.00
β [°]	101.954(2)	107.7380(10)
γ [°]	90.124(2)	90.00
V [Å^3]	911.31(5)	3424.8(4)
Z	2	4
T [K]	293	293
$\rho_{calcd.}$ [g cm^{-3}]	1.731	1.771
μ [mm^{-1}]	1.850	2.812
F [000]	478	1772
Total reflections	3177	7895
Reflections observed	2789	5453
Parameters	236	379
Goodness-of-fit on F^2	1.091	1.035
$R1$[a] [$I > 2\sigma(I)$]	0.0694	0.0697
wR[b] [$I > 2\sigma(I)$]	0.2061	0.2265
Max. peak/hole [e Å^{-3}]	1.583/– 0.937	2.844/–1.054

[a] $R1 = (\Sigma||F_o| - |F_c||)/(\Sigma|F_o|)$. [b] $wR2 = [\Sigma w(F_o^2 - F_c^2)^2/\Sigma w(F_o^2)^2]^{1/2}$.

CCDC-293055 (for **3**) and -289306 (for **5**) contain the supplementary crystallographic data for this paper. These data can be obtained free of charge from The Cambridge Crystallographic Data Center via www.ccdc.cam.ac.uk/data_request/cif.

Computational Methods: The density functional theory (DFT) method was used to optimize the isomeric geometries of complex **5**. Calculations were performed with the B3LYP functional[49] included in the Gaussian 03 program package.[50] The D95 basis set[51] was used for all atoms except Fe and I, for which the LANL2DZ basis set[52] was used with the effective core potential (ECP) of LANL2DZ. The effect of solvent on the stability of the isomers was considered by optimizing all the geometries in CCl_4 solution using the PCM method[53] included in Gaussian 03.

Electrochemistry: Acetonitrile used for electrochemical measurements was distilled once from CaH_2 and once from P_2O_5 and freshly distilled from CaH_2 under N_2. Measurements were made with a BAS 100B electrochemical workstation. All cyclic voltammograms were obtained in a conventional three-electrode cell under argon and at ambient temperature. The working electrode was a glassy carbon electrode (diameter 3 mm) that was successively polished with 3-μm and 1-μm alumina pastes and sonicated in ion-free water for 15 min prior to use. The supporting electrolyte was 0.1 M nBu$_4$NPF$_6$ (Fluka, electrochemical grade). The experimental reference electrode was a nonaqueous Ag/Ag$^+$ electrode (0.01 M $AgNO_3$/0.1 M nBu$_4$NPF$_6$ in CH_3CN). Ferrocene was used as an internal standard. All potentials reported in this paper are relative to the Fc$^+$/Fc couple. The counter electrode was platinum wire. During the electrocatalytic experiments under argon, increments of acid were added by microsyringe. Bulk electrolysis experiments were performed under argon with a BAS 100 B/W electrochemical analyzer, which was carried out on a glassy carbon rod (A = 3.14 cm^2) in a gas-tight H-type electrolysis cell containing about 14 mL of CH_3CN solution. Gas chromatography was performed with a GC 920 instrument equipped with a thermal conductivity detector (TCD) under isothermal conditions with argon as carrier gas.

Supporting Information (see also the footnote on the first page of this article): Energetic properties of isomers of complex **5** calculated both in the gas phase and CCl_4 solution using PCM method. Geometrical bond lengths and angles calculated for the isomers **5.1**–**5.4**.

Acknowledgments

We are grateful to the Ministry of Education of China and the National Natural Science Foundation of China (projects 20128005, 20376010, and 20472012). We also thank the Supercomputing Center of CNIC (CAS) for the support of calculations.

[1] M. W. W. Adam, *Biochim. Biophys. Acta* **1990**, *1020*, 115–145.
[2] J. W. Peters, *Curr. Opin. Struct. Biol.* **1999**, *9*, 670–676.
[3] M. Frey, *ChemBioChem* **2002**, *3*, 152–160.
[4] J. W. Peters, W. N. Lanzilotta, B. J. Lemon, L. C. Seefeldt, *Science* **1998**, *282*, 1853–1858.
[5] Y. Nicolet, C. Piras, P. Legrand, C. E. Hatchikian, J. C. Fontecilla-Camps, *Structure* **1999**, *7*, 13–23.
[6] A. L. De Lacey, C. Stadler, C. Cavazza, E. C. Hatchikian, V. M. Fernandez, *J. Am. Chem. Soc.* **2000**, *122*, 11232–11233.
[7] Z. Chen, B. J. Lemon, S. Huang, D. J. Swartz, J. W. Peters, K. A. Bagley, *Biochemistry* **2002**, *41*, 2036–2043.
[8] Y. Nicolet, A. L. de Lacey, X. Vernède, V. M. Fernandez, E. C. Hatchikian, J. C. Fontecilla-Camps, *J. Am. Chem. Soc.* **2001**, *123*, 1596–1601.
[9] H.-J. Fan, M. B. Hall, *J. Am. Chem. Soc.* **2001**, *123*, 3828–3829.
[10] M. Y. Darensbourg, *Nature* **2005**, *433*, 589–591.
[11] M. Y. Darensbourg, E. J. Lyon, J. J. Smee, *Coord. Chem. Rev.* **2000**, *206–207*, 533–561.
[12] M. Y. Darensbourg, E. J. Lyon, X. Zhao, I. P. Georgakaki, *Proc. Natl. Acad. Sci. USA* **2003**, *7*, 3683–3688.
[13] D. J. Evans, C. J. Pickett, *Chem. Soc. Rev.* **2003**, *32*, 268–275.
[14] T. B. Rauchfuss, *Inorg. Chem.* **2004**, *43*, 14–26.
[15] L. Sun, B. Åkermark, S. Ott, *Coord. Chem. Rev.* **2005**, *249*, 1653–1663.
[16] E. J. Lyon, I. P. Georgakaki, J. H. Reibenspies, M. Y. Darensbourg, *Angew. Chem. Int. Ed.* **1999**, *38*, 3178–3180.

[17] J. D. Lawrence, H. Li, T. B. Rauchfuss, M. Bénard, M.-M. Rohmer, *Angew. Chem. Int. Ed.* **2001**, *40*, 1768–1771.
[18] H. Li, T. B. Rauchfuss, *J. Am. Chem. Soc.* **2002**, *124*, 726–727.
[19] J. D. Lawrence, T. B. Rauchfuss, S. R. Wilson, *Inorg. Chem.* **2002**, *41*, 6193–6195.
[20] J. L. Nehring, D. M. Heinekey, *Inorg. Chem.* **2003**, *42*, 4288–4292.
[21] M. Razavet, S. C. Davies, D. L. Hughes, C. J. Pickett, *Chem. Commun.* **2001**, 847–848.
[22] S. J. George, Z. Cui, M. Razavet, C. J. Pickett, *Chem. Eur. J.* **2002**, *8*, 4037–4046.
[23] L. Song, Z. Yang, H. Bian, Q. Hu, *Organometallics* **2004**, *23*, 3082–3084.
[24] E. J. Lyon, I. P. Georgakaki, J. H. Reibenspies, M. Y. Darensbourg, *J. Am. Chem. Soc.* **2001**, *123*, 3268–3278.
[25] F. Gloaguen, J. D. Lawrence, M. Schmidt, S. R. Wilson, T. B. Rauchfuss, *J. Am. Chem. Soc.* **2001**, *123*, 12518–12527.
[26] C. Tard, X. Liu, S. K. Ibrahim, M. Bruschi, L. D. Gioia, S. C. Davies, X. Yang, L.-S. Wang, G. Sawers, C. J. Pickett, *Nature* **2005**, *433*, 610–613.
[27] C. A. Boyke, T. B. Rauchfuss, S. R. Wilson, M.-M. Rohmer, M. Bénard, *J. Am. Chem. Soc.* **2004**, *126*, 15151–15160.
[28] C. A. Boyke, J. I. van der Vlugt, T. B. Rauchfuss, S. R. Wilson, G. Zampella, L. De Gioia, *J. Am. Chem. Soc.* **2005**, *127*, 11010–11018.
[29] D. Chong, I. P. Georgakaki, R. Mejia-Rodriguez, J. Sanabria-Chinchilla, M. P. Soriaga, M. Y. Darensbourg, *Dalton Trans.* **2003**, 4158–4163.
[30] R. Mejia-Rodriguez, D. Chong, J. H. Reibenspies, M. P. Soriaga, M. Y. Darensbourg, *J. Am. Chem. Soc.* **2004**, *126*, 12004–12014.
[31] F. Gloaguen, J. D. Lawrence, T. B. Rauchfuss, *J. Am. Chem. Soc.* **2001**, *123*, 9476–9477.
[32] F. Gloaguen, J. D. Lawrence, T. B. Rauchfuss, M. Bénard, M.-M. Rohmer, *Inorg. Chem.* **2002**, *41*, 6573–6582.
[33] S. Ott, M. Kritikos, B. Åkermark, L. Sun, R. Lomoth, *Angew. Chem. Int. Ed.* **2004**, *43*, 1006–1009.
[34] J. D. Lawrence, H. Li, T. B. Rauchfuss, *Chem. Commun.* **2001**, 1482–1483.
[35] T. Liu, M. Wang, Z. Shi, H. Cui, W. Dong, J. Chen, B. Åkermark, L. Sun, *Chem. Eur. J.* **2004**, *10*, 4474–4479.
[36] S. Ott, M. Borgström, M. Kritikos, R. Lomoth, J. Bergquist, B. Åkermark, L. Hammarström, L. Sun, *Inorg. Chem.* **2004**, *43*, 4683–4692.
[37] F. Wang, M. Wang, X. Liu, K. Jin, W. Dong, G. Li, B. Åkermark, L. Sun, *Chem. Commun.* **2005**, 3221–3223.
[38] W. Dong, M. Wang, X. Liu, K. Jin, G. Li, F. Wang, L. Sun, *Chem. Commun.* **2006**, 305–307.
[39] L. Schwartz, G. Eilers, L. Eriksson, A. Gogoll, R. Lomoth, S. Ott, *Chem. Commun.* **2006**, 520–522.
[40] D. Seyferth, R. S. Henderson, L. C. Song, *Organometallics* **1982**, *1*, 125–133.
[41] I. Bhugun, D. Lexa, J.-M. Savéant, *J. Am. Chem. Soc.* **1996**, *118*, 3982–3983.
[42] The different reference systems were compared by using [(μ-PDT)$Fe_2(CO)_6$] as a calibrating agent, which is reduced at –1.16 V vs. Ag/AgCl (see ref. 25). With our system, and under the same conditions, the complex is reduced at –1.65 V, which gives a ΔE value of 0.49 V.
[43] H.-J. Fan, M. B. Hall, *J. Am. Chem. Soc.* **2001**, *123*, 3828–3829.
[44] S. J. Borg, T. Behrsing, S. P. Best, M. Razavet, X. Liu, C. J. Pickett, *J. Am. Chem. Soc.* **2004**, *126*, 16988–16999.
[45] D. Seyferth, R. S. Henderson, *J. Organomet. Chem.* **1981**, *218*, C34–C36.
[46] R. Obreht, R. Herrmann, I. Ugi, *Synthesis* **1985**, 400–402.
[47] SMART and SAINT, Siemens Analytical X-ray Instruments Inc., Madison, WI, USA, **1996**.
[48] SHELXTL, Version 5.1, Siemens Industrial Automation, Inc., **1997**.
[49] A. D. Becke, *J. Chem. Phys.* **1993**, *98*, 5648–5652.
[50] M. J. Frisch, G. W. Trucks, H. B. Schlegel, G. E. Scuseria, M. A. Robb, J. R. Cheeseman, J. A. Montgomery Jr, T. Vreven, K. N. Kudin, J. C. Burant, J. M. Millam, S. S. Iyengar, J. Tomasi, V. Barone, B. Mennucci, M. Cossi, G. Scalmani, N. Rega, G. A. Petersson, H. Nakatsuji, M. Hada, M. Ehara, K. Toyota, R. Fukuda, J. Hasegawa, M. Ishida, T. Nakajima, Y. Honda, O. Kitao, H. Nakai, M. Klene, X. Li, J. E. Knox, H. P. Hratchian, J. B. Cross, C. Adamo, J. Jaramillo, R. Gomperts, R. E. Stratmann, O. Yazyev, A. J. Austin, R. Cammi, C. Pomelli, J. W. Ochterski, P. Y. Ayala, K. Morokuma, G. A. Voth, P. Salvador, J. J. Dannenberg, V. G. Zakrzewski, S. Dapprich, A. D. Daniels, M. C. Strain, O. Farkas, D. K. Malick, A. D. Rabuck, K. Raghavachari, J. B. Foresman, J. V. Ortiz, Q. Cui, A. G. Baboul, S. Clifford, J. Cioslowski, B. B. Stefanov, G. Liu, A. Liashenko, P. Piskorz, I. Komaromi, R. L. Martin, D. J. Fox, T. Keith, M. A. Al-Laham, C. Y. Peng, A. Nanayakkara, M. Challacombe, P. M. W. Gill, B. Johnson, W. Chen, M. W. Wong, C. Gonzalez, and J. A. Pople, *Gaussian 03*, Revision C.02, Gaussian, Inc., Wallingford CT, **2004**.
[51] T. H. Dunning Jr, P. J. Hay, in *Modern Theoretical Chemistry* (Ed.: H. F. Schaefer III), vol. 3, Plenum, New York, **1976**, 1–28.
[52] P. J. Hay, W. R. Wadt, *J. Chem. Phys.* **1985**, *82*, 270–283; W. R. Wadt, P. J. Hay, *J. Chem. Phys.* **1985**, *82*, 284–298; P. J. Hay, W. R. Wadt, *J. Chem. Phys.* **1985**, *82*, 299–310.
[53] M. T. Cancès, B. Mennucci, J. Tomasi, *J. Chem. Phys.* **1997**, *107*, 3032–3041.

Received: May 15, 2006
Published Online: September 18, 2006

